Science Signaling
AAAS

stke.sciencemag.org/cgi/content/full/12/604/eaaw5573/DC1

Supplementary Materials for

Induction of metabolic quiescence defines the transitional to follicular B cell switch

Jocelyn R. Farmer, Hugues Allard-Chamard, Na Sun, Maimuna Ahmad, Alice Bertocchi, Vinay S. Mahajan, Toby Aicher, Johan Arnold, Mark D. Benson, Jordan Morningstar, Sara Barmettler, Grace Yuen, Samuel J. H. Murphy, Jolan E. Walter, Musie Ghebremichael, Alex K. Shalek, Facundo Batista, Robert Gerszten, Shiv Pillai*

*Corresponding author. Email: pillai@helix.mgh.harvard.edu

Published 22 October 2019, *Sci. Signal.* **12**, eaaw5573 (2019)
DOI: 10.1126/scisignal.aaw5573

This PDF file includes:

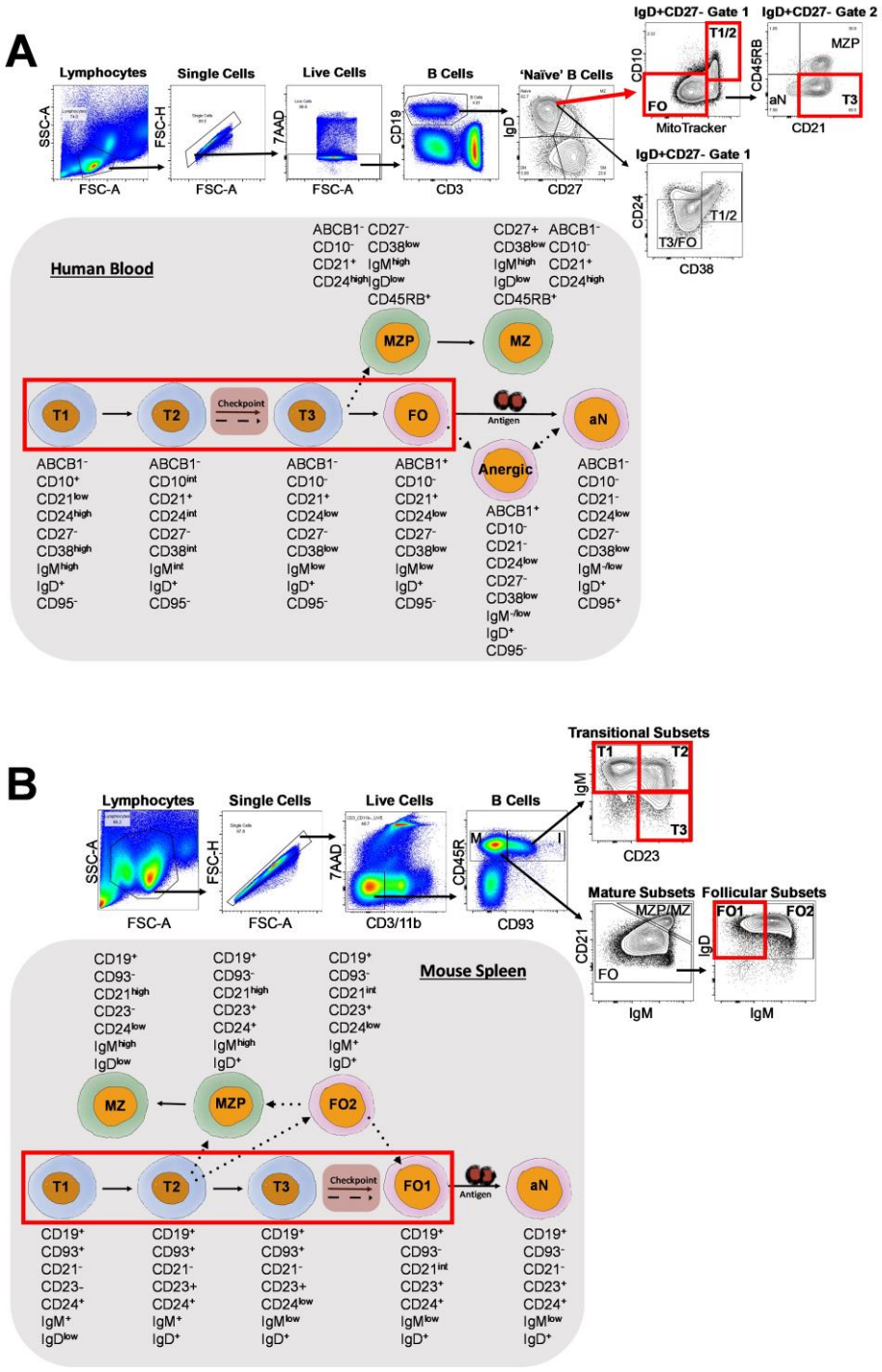

Fig. S1. B cell gating strategy. Flow cytometry gating strategy (top) and schematic of marker expression (bottom) of human **(A)** and mouse **(B)** B cells at given maturation stages. Arrows indicate established (solid) or hypothesized (dotted) maturation potential. Red boxes indicated gating strategy used in this manuscript. Activated naïve (aN), FO, immature (I), marginal zone (MZ), marginal zone precursor (MZP), mature (M), T1-3.

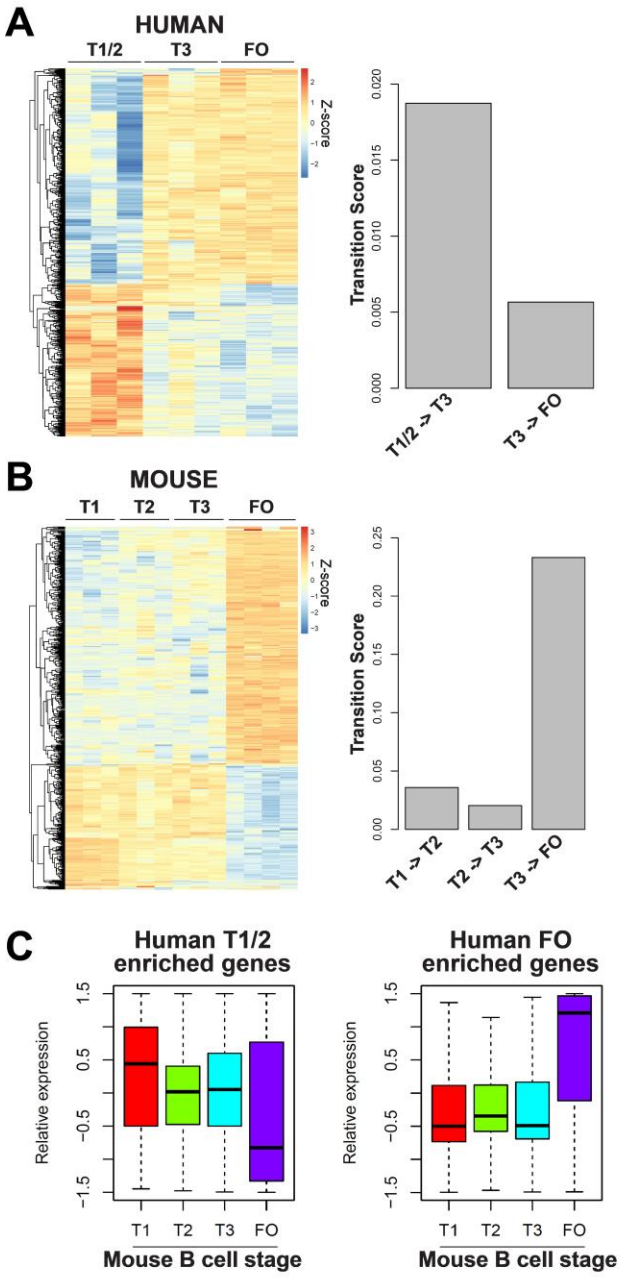

Fig. S2. The major transcriptional checkpoint occurs at the transitional T3 B cell stage in human versus the FO B cell stage in mouse. (**A** to **C**) RNA-sequencing analysis of whole gene expression in sorted populations of transitional (T1/2 and T3) and follicular (FO) human B cells (A), compared to transitional (T1, T2, and T3) and follicular (FO) mouse B cells (B). Heat maps of all differentially expressed genes in human and mouse B cells at distinct maturation stages (left), transition scores of the total number of differentially expressed genes at each stage (right), and relative differential gene expression of human genes in the mice (C) are from ≥ 3 biological replicates.

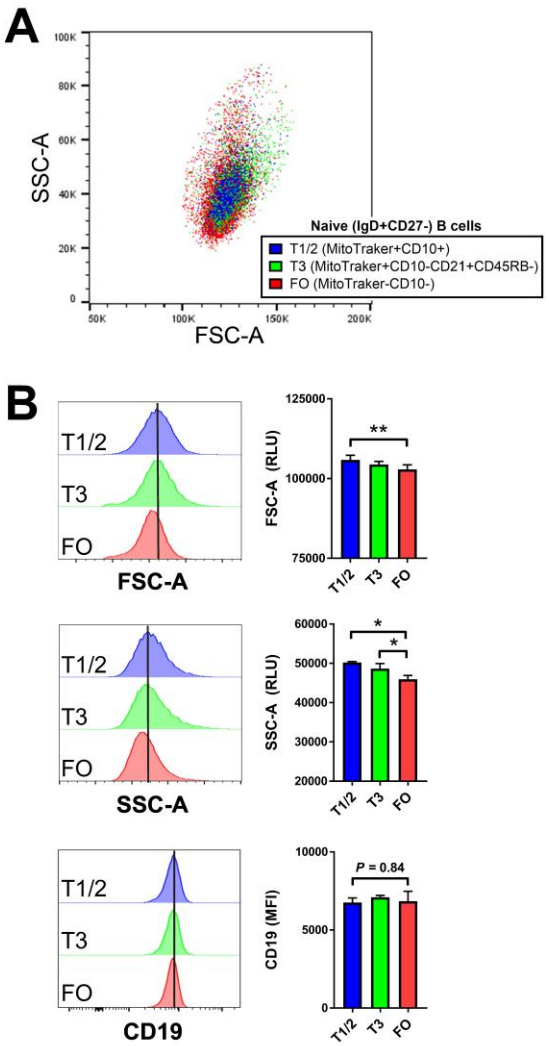

Fig. S3. Transitional and FO human B cells analyzed by flow cytometry demonstrate comparable B cell surface protein amounts despite differences in forward and side scatter. (**A** and **B**) Flow cytometry analysis of cell size, granularity, and CD19 abundance in B cell subsets as indicated. Dot plot and histograms are representative of 3 biological replicates. Quantified data (right) are means +/- SD of all replicates. **P*<0.05 and ***P*<0.005 by paired Student's t-test.

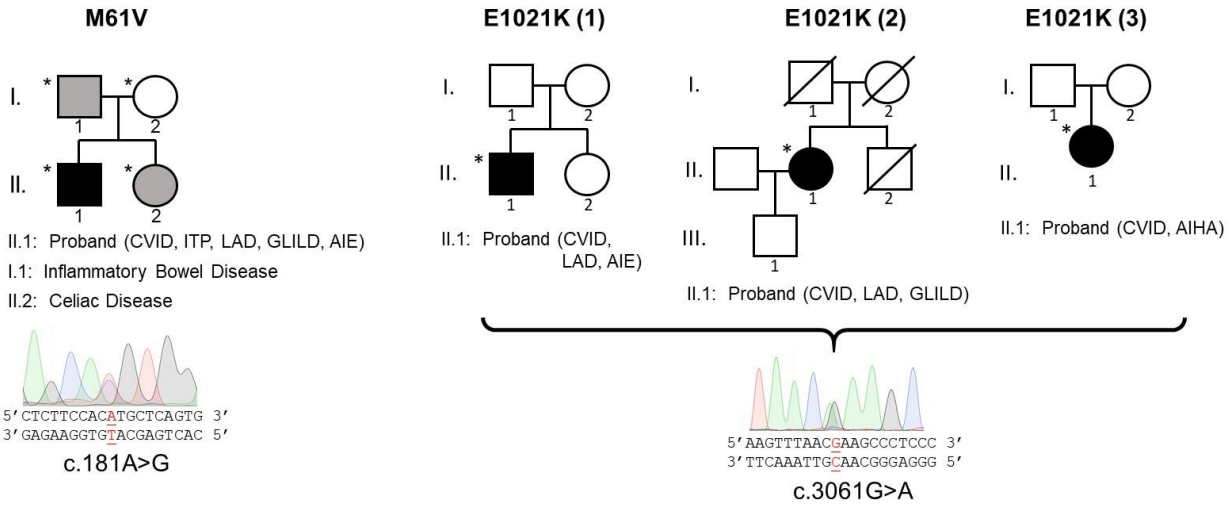

Fig. S4. Patients identified with activating mutations in *PIK3CD*. (Top) Pedigrees of proband (black), carrier family members (grey), and all sequenced family members (*) with clinical description of the affected patients (autoimmune enteropathy (AIE), autoimmune hemolytic anemia (AIHA), common variable immunodeficiency (CVID), granulomatous lymphointerstitial lung disease (GLILD), immune thrombocytopenia purpura (ITP), lymphadenopathy (LAD)). (Bottom) Sanger sequencing of the germline *PIK3CD* locus. Data are from the 4 patients described in Table S1.

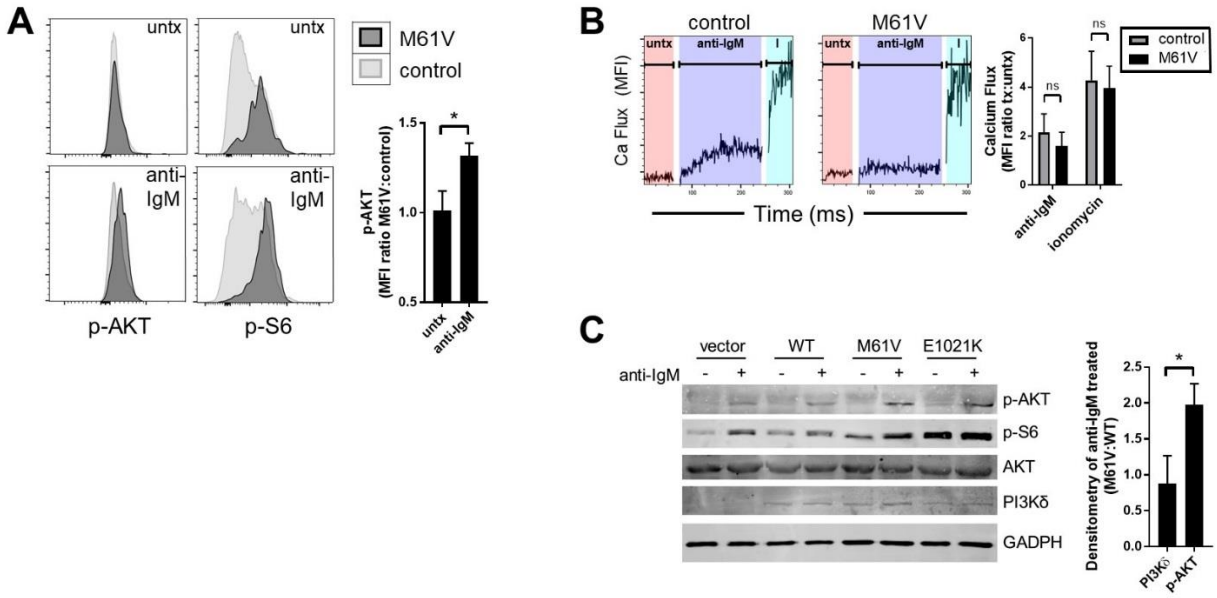

Fig. S5. The *PIK3CD* M61V mutation promotes BCR-stimulated AKT and S6 activation. (**A**) Phospho-flow cytometry analysis of pAKT and pS6 amounts in total (CD19+) peripheral B cells from control and M61V patient samples after anti-IgM treatment for 5-10 minutes, as indicated. Histograms are representative of 3 biological replicates/group. Quantified data are means +/- SD of three biological replicates/group. (**B**) Flow cytometry analysis of intracellular calcium signaling in total (CD19+) peripheral B cells from control and M61V patient samples after anti-IgM for 5 minutes, as indicated. Plots (left) are representative of 3 biological replicates/group. Quantified data are means +/- SD of 3 biological replicates/group. (**C**) Immunoblot analysis of pAKT and pS6 amounts in whole cell lysates of Ramos cells transduced with the indicated PI3Kδ constructs and treated with anti-IgM for 5 minutes, as indicated. Blots are representative of 3 biological replicates/group. Quantified data are means +/- SD of three biological replicates/group. **P*<0.05, ns=not statistically different by unpaired Student's t-test.

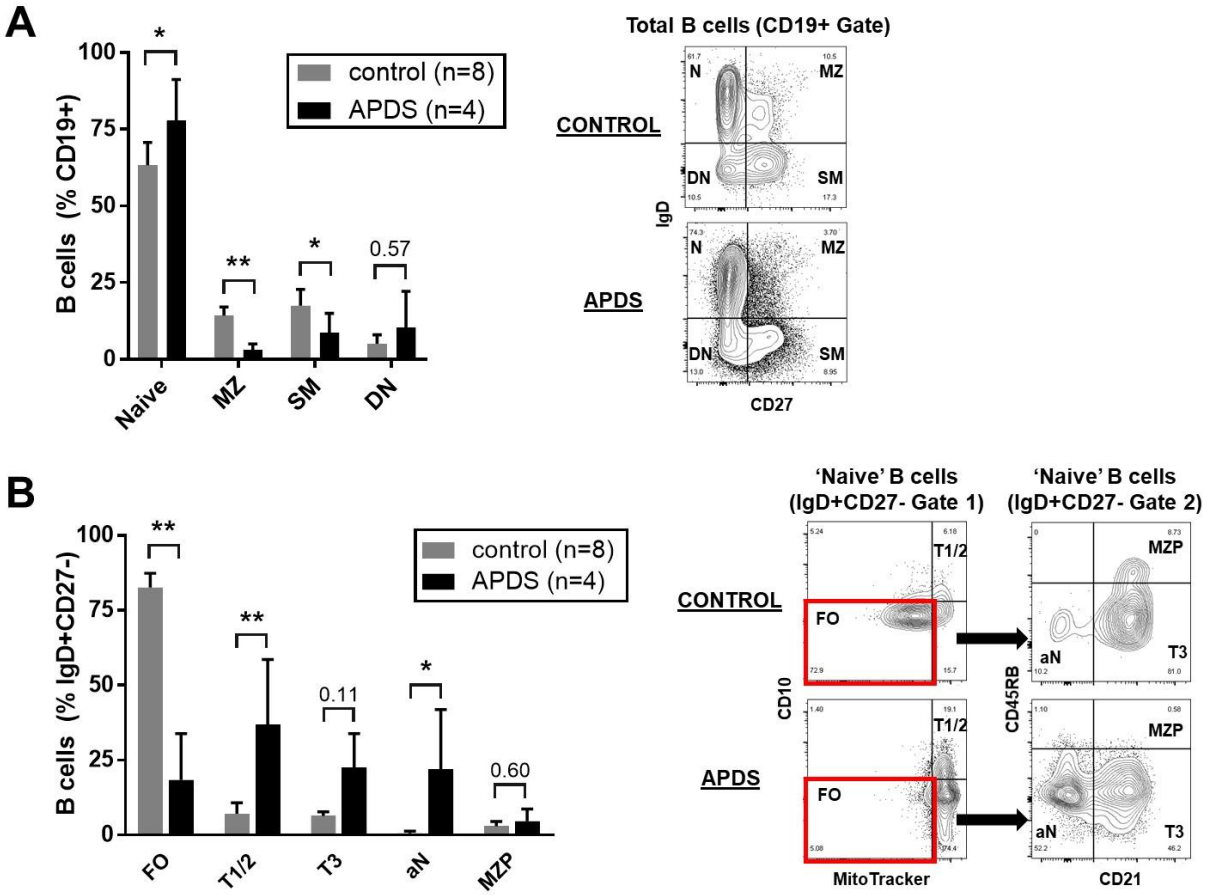

Fig. S6. FO B cell development is blocked in patients with gain-of-function *PIK3CD* (PI3Kδ) mutations. (**A** and **B**) Total naïve (N), marginal zone (MZ), switched-memory (SM), and double negative (DN) CD19+ B cell subsets (A) and follicular (FO), transitional (T), activated naïve (aN), and marginal zone precursor (MZP) IgD+CD27- B cell subsets (B) in healthy controls and activating PI3Kδ syndrome (APDS) patients. Dot plots (right) are representative of ≥ 4 biological replicates/group. Quantified data (left) are means +/- SD of all samples. **P*<0.05, and ***P*<0.005 by Mann-Whitney test.

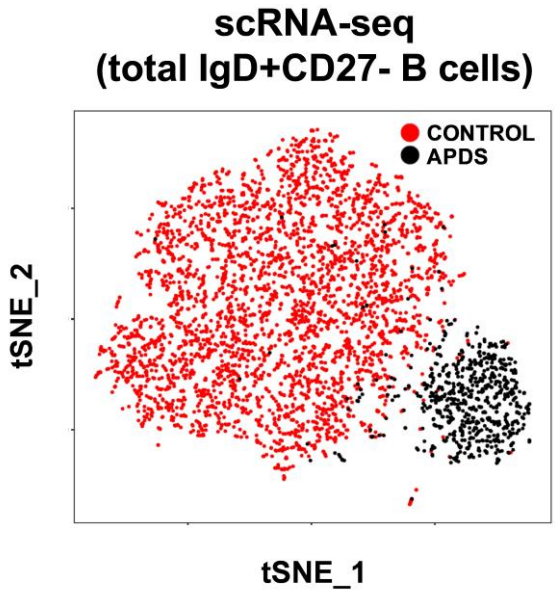

Fig. S7. APDS naïve ($IgD^{+}CD27^{-}$) B cells cluster unique from healthy controls by scRNA-seq analysis using t-SNE. Single-cell RNA-sequencing of total IgD+CD27- B cells in healthy controls (red) and APDS patient (black). t-SNE analysis is from one APDS patient and three healthy controls (see also Fig. 3C).

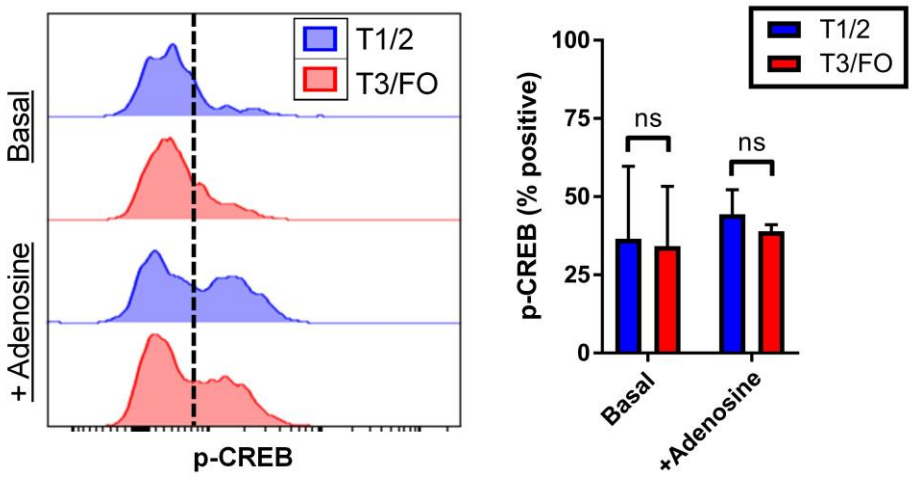

Fig. S8. cAMP signaling is similar between early transitional and late transitional/FO B cells. Phospho-flow cytometry analysis of pCREB amounts in T1/2 and T3/FO B cell subsets at baseline and after stimulation with adenosine for 60 minutes. Histograms (left) are representative of 3 biological replicates/group. Quantified data (right) are means +/- SD of three biological replicates/group. Ns=not significant by paired Student's t-test.

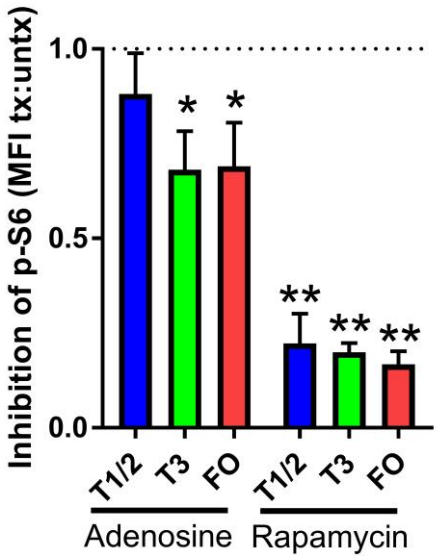

Fig. S9. Adenosine is sufficient to inhibit pS6 activation in transitional T3 and FO B cells. Phospho-flow cytometry analysis of pS6 amounts in sorted T1/2, T3, and FO B cell subsets at baseline or after stimulation with adenosine or rapamycin for 60 minutes, as indicated. Quantified data are means +/- SD presented as ratio of pS6 MFI in treated (tx) to untreated (untx) samples for three biological replicates/group. *P<0.05, **P<0.005 by unpaired Student's t-test to untreated.

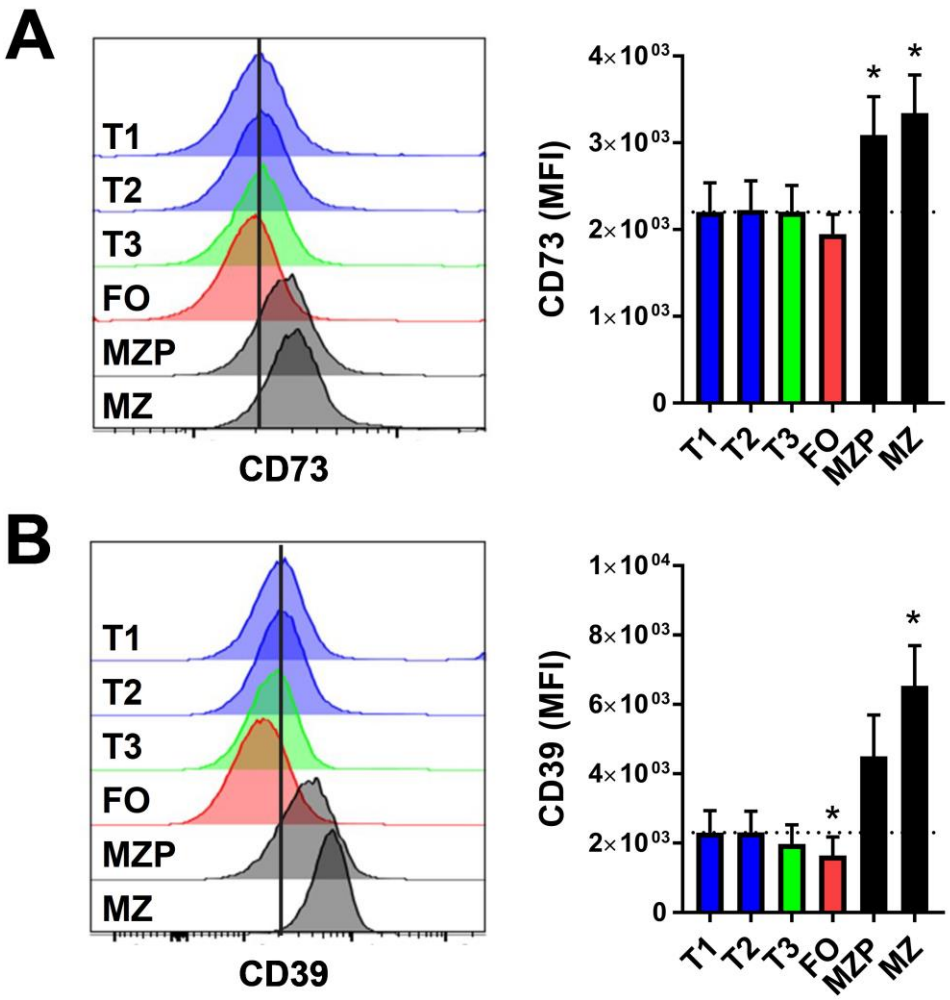

Fig. S10. Increased abundance of cell surface ectonucleotidases at the FO B cell stage is not conserved between human and mouse. (**A** and **B**) Flow cytometry analysis of cell surface amounts of ectonucleotidases CD73 (A) and CD39 (B) on B cell subsets from mouse spleen. Histograms (left) are representative of three biological replicates. Quantified data (right) are means +/- SD of three biological replicates. T1 mean indicated by dotted line. **P*<0.05 by paired Student's t-test to T1.

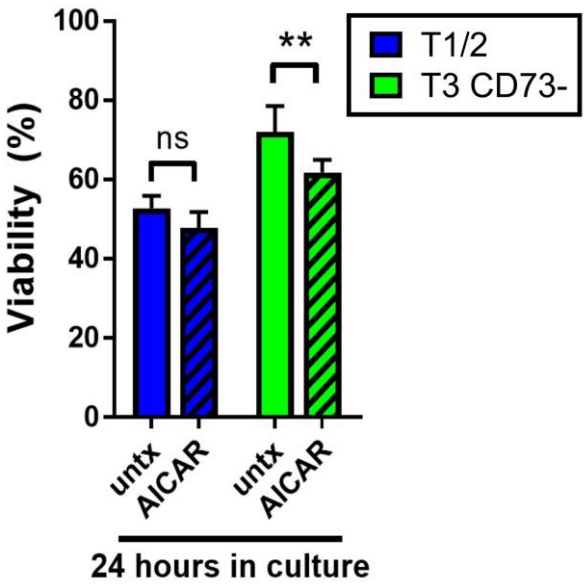

Fig. S11. B cell viability in vitro. Cell viability by flow cytometric assessment of 7-aminoactinomycin D (7-AAD) positivity in untreated (untx) and AICAR treated human B cell subsets, as indicated, at 24 hours in culture. Quantified data are means +/- SD of six biological replicates/group. $^{**}P<0.005$ and ns=not significant by unpaired Student's t-test.

Table S1. Top gene set enrichment pathways for transitional to FO B cell development.

HUMAN			
Enriched Hallmark Gene Sets (all)	**Term**	**Pattern**	***P* value**
hallmark_myc_targets_v1	MYC_TARGETS_V1	decreased in T3/FO	2.75E-08
hallmark_oxidative_phosphorylation	OXIDATIVE_PHOSPHORYLATION	decreased in T3/FO	5.79E-06
hallmark_unfolded_protein_response	UNFOLDED_PROTEIN_RESPONSE	decreased in T3/FO	0.0001794
hallmark_pi3k_akt_mtor_signaling	PI3K_AKT_MTOR_SIGNALING	decreased in T3/FO	0.0039326
hallmark_heme_metabolism	HEME_METABOLISM	decreased in T3/FO	0.0069661
hallmark_mtorc1_signaling	MTORC1_SIGNALING	decreased in T3/FO	0.0080747
Enriched GO Gene Sets (top 24)	**Term**	**Pattern**	***P* value**
GO:0043043	peptide biosynthetic process	decreased in T3/FO	6.52E-21
GO:0006412	translation	decreased in T3/FO	6.60E-21
GO:0043604	amide biosynthetic process	decreased in T3/FO	5.33E-19
GO:0006518	peptide metabolic process	decreased in T3/FO	9.96E-19
GO:0006413	translational initiation	decreased in T3/FO	2.34E-18
GO:0006613	cotranslational protein targeting to membrane	decreased in T3/FO	3.83E-17
GO:0006614	SRP-dependent cotranslational protein targeting to membrane	decreased in T3/FO	1.60E-16
GO:0019080	viral gene expression	decreased in T3/FO	2.10E-16
GO:0019083	viral transcription	decreased in T3/FO	4.64E-16
GO:0045047	protein targeting to ER	decreased in T3/FO	8.01E-16
GO:0072599	establishment of protein localization to endoplasmic reticulum	decreased in T3/FO	1.69E-15
GO:0043603	cellular amide metabolic process	decreased in T3/FO	2.59E-15
GO:0006612	protein targeting to membrane	decreased in T3/FO	3.14E-15
GO:0070972	protein localization to endoplasmic reticulum	decreased in T3/FO	3.49E-15
GO:0044033	multi-organism metabolic process	decreased in T3/FO	3.53E-15
GO:0000184	nuclear-transcribed mRNA catabolic process, nonsense-mediated decay	decreased in T3/FO	1.33E-14
GO:1901566	organonitrogen compound biosynthetic process	decreased in T3/FO	2.93E-14
GO:1901564	organonitrogen compound metabolic process	decreased in T3/FO	2.75E-13
GO:0019058	viral life cycle	decreased in T3/FO	4.63E-13
GO:0006396	RNA processing	decreased in T3/FO	8.06E-13
GO:0016071	mRNA metabolic process	decreased in T3/FO	1.28E-12
GO:0000956	nuclear-transcribed mRNA catabolic process	decreased in T3/FO	1.65E-12
GO:0090150	establishment of protein localization to membrane	decreased in T3/FO	2.98E-12
GO:0042254	ribosome biogenesis	decreased in T3/FO	3.71E-12
MOUSE			
Enriched Hallmark Gene Sets (all)	**Term**	**Pattern**	***P* value**
hallmark_mtorc1_signaling	MTORC1_SIGNALING	decreased in FO	3.60E-08
hallmark_oxidative_phosphorylation	OXIDATIVE_PHOSPHORYLATION	decreased in FO	3.07E-06
hallmark_myc_targets_v1	MYC_TARGETS_V1	decreased in FO	3.46E-05
hallmark_allograft_rejection	ALLOGRAFT_REJECTION	decreased in FO	0.0004471
hallmark_pi3k_akt_mtor_signaling	PI3K_AKT_MTOR_SIGNALING	decreased in FO	0.0014784
hallmark_glycolysis	GLYCOLYSIS	decreased in FO	0.0024929
Enriched GO Gene Sets (top 24)	**Term**	**Pattern**	***P* value**
GO:0006412	translation	decreased in FO	1.94E-28
GO:0043043	peptide biosynthetic process	decreased in FO	9.61E-28
GO:0006518	peptide metabolic process	decreased in FO	9.45E-26
GO:0043604	amide biosynthetic process	decreased in FO	2.11E-25
GO:1901564	organonitrogen compound metabolic process	decreased in FO	9.56E-24
GO:0043603	cellular amide metabolic process	decreased in FO	1.06E-22

GO:1901566	organonitrogen compound biosynthetic process	decreased in FO	1.08E-22
GO:0044267	cellular protein metabolic process	decreased in FO	3.86E-14
GO:0034641	cellular nitrogen compound metabolic process	decreased in FO	2.71E-13
GO:0006807	nitrogen compound metabolic process	decreased in FO	9.55E-13
GO:0019538	protein metabolic process	decreased in FO	1.90E-12
GO:0010467	gene expression	decreased in FO	3.97E-12
GO:0044271	cellular nitrogen compound biosynthetic process	decreased in FO	1.32E-11
GO:1901576	organic substance biosynthetic process	decreased in FO	1.39E-10
GO:0042254	ribosome biogenesis	decreased in FO	1.90E-10
GO:0009058	biosynthetic process	decreased in FO	2.56E-10
GO:0044249	cellular biosynthetic process	decreased in FO	2.98E-10
GO:0044237	cellular metabolic process	decreased in FO	3.73E-10
GO:0034645	cellular macromolecule biosynthetic process	decreased in FO	8.90E-10
GO:0022613	ribonucleoprotein complex biogenesis	decreased in FO	1.11E-09
GO:0009059	macromolecule biosynthetic process	decreased in FO	1.16E-09
GO:0008152	metabolic process	decreased in FO	4.51E-09
GO:0002181	cytoplasmic translation	decreased in FO	7.60E-09
GO:0071704	organic substance metabolic process	decreased in FO	8.15E-09

Table S2. Characteristics of patients with APDS.

***PIK3CD* Mutation**	p.E1021K (1)	p.E1021K (2)	p.E1021K (3)	p.M61V
Age at B cell phenotyping	28 years	47 years	12 years	28 years
Gender	M	F	F	M
Infections	sino-pulmonary	sino-pulmonary, HPV	sino-pulmonary	sino-pulmonary, VZV
Lymphoproliferation	LAD, AIE splenomegaly	LAD, GLILD splenomegaly	splenomegaly	LAD, GLILD, AIE, splenomegaly
Autoimmunity	-	-	AIHA	ITP
Bronchiectasis	-	+	+	+
ALC (1000-4800 cells/μL)	570-980	1770	n/a	270-950
CD3+ (690-2540 cells/μL)	732	1434	885	495
CD4+ (419-1590 cells/μL)	226	n/a	347	211
CD4+CD45RA+ (% CD4+)	8.1%	n/a	12.7%	3.0%
CD4+CD45RO+ (% CD4+)	89.4%	n/a	n/a	87.8%
CD8+ (190-1140 cells/μL)	465	n/a	494	259
CD8+CD45RA+ (% CD8+)	56.2%	n/a	10.7%	57.6%
CD8+CD45RO+ (% CD8+)	34.3%	n/a	n/a	15.4%
CD19+ (90-660 cells/μL)	136	142	285	77
CD3-CD16/56+ (90-590 cells/μL)	122	160	139	40
IgG (614-1295 mg/dL)	*replaced	445	*replaced	87-183
IgA (69-309 mg/dL)	64-119	5-116	182	13-19
IgM (53-334 mg/dL)	284-420	641-1552	382	388-1350
Pneumococcal titers (≥1.3 μg/mL)	10/23+ (post-pneumovax)	0/14+ (post-pneumovax)	n/a	0/23+ (post-pneumovax)
Treatment prior to B cell phenotyping	SCIG	IVIG	SCIG	SCIG; rituximab

Normal reference ranges from the Massachusetts General Hospital shown where applicable. Pneumococcal titers shown as ratio of positive over tested serotypes. Autoimmune enteropathy (AIE); autoimmune hemolytic anemia (AIHA); immune thrombocytopenia (ITP); intravenous immunoglobulin (IVIG); female (F); granulomatous-lymphointerstitial lung disease (GLILD); human papilloma virus (HPV); lymphadenopathy (LAD); male (M); not available (n/a); subcutaneous immunoglobulin (SCIG); varicella zoster virus (VZV).

Table S3. Primers used for generating the WT, E1021K, and M61V mutant PI3Kδ constructs.

Name	Sequence (5'-->3')	Annealing Temp (ºC)
1: PI3KD_FOR	agctggcctctgaggccaccATGCCCCCTGGGGTGGA	70.8
2: PI3KD_REV	cgtgtccaaagacaacaggcagtagggcctgtcaggccaagcttg	70.8
3: E1021K_N_FOR	tcgagtccaaccctgggcccATGCCCCCTGGGGTGGAC	70.1
4: E1021K_N_REV	GTTAAACTTCACTCGGAAGTGCTTCAGTG	70.1
5: E1021K_C_FOR	ttccgagtgaagtttaacAAAGCCCTCCGTGAGAGC	64.1
6: E1021k_C_REV	aaacggcgcgccgcggccgcCTACTGCCTGTTGTCTTTGG	64.1
7: M61V_N_FOR	tcgagtccaaccctgggcccATGCCCCCTGGGGTGGAC	71.1
8: M61V_N_REV	cactgagcacGTGGAAGAGCGGCTCATACTGG	71.1
9: M61V_C_FOR	gctcttccacGTGCTCAGTGGCCCCGAG	68.7
10: M61V_C_REV	aaacggcgcgccgcggccgcCTACTGCCTGTTGTCTTTGGACAC	68.7
11: PsBbi-GP_FOR	GGTGGCCTCAGAGGCCAG	72
12: PSBbi-GP_REV	GGCCTGTCAGGCCAAGCT	72